Journal of Materials Chemistry B

Accepted Manuscript

ROYAL SOCIETY OF CHEMISTRY

www.rsc.org/materialsB

Journal Name Journal of Materials Chemistry B Dynamic Article Links ►

Cite this: DOI: 10.1039/c0xx00000x

www.rsc.org/xxxxxx

ARTICLE TYPE

New Biocompatible Polymeric Micelles Designed for Efficient Intracellular Uptake and Delivery

Francesca Di Maria,[a] Laura Blasi,[b] Alessandra Quarta,[b] Giacomo Bergamini,[c] Giovanna Barbarella,[a] Loris Giorgini[d] and Massimo Benaglia*[a]

Received (in XXX, XXX) Xth XXXXXXXXX 20XX, Accepted Xth XXXXXXXXX 20XX
DOI: 10.1039/b000000x

New amphiphilic block copolymers are easily synthesised by post-polymerisation modifications of poly(glycidyl methacrylate) chains derivatives. The obtained material, upon dispersion in water, is capable of self-assembling into robust micelles. These nanoparticles, which are also characterised by adaptable stability, were loaded with different thiophene based fluorophores. The photoluminescent micelles were administered to cultured cells revealing a high and rapid internalisation of structurally different fluorescent molecules by the same internalisation pathway. Appropriate pairs of chromophores were selected and loaded into the micelles to induce Förster resonance energy transfer (FRET). The disappearing of the FRET phenomenon, after cells uptaking, demonstrated the intracellular release of the nanoparticles contents. The studied nanomaterial and the loaded chromophores have also shown to be biocompatible and non toxic towards the tested cells.

Introduction

The construction of functional materials in nature is always governed by self-assembling processes. Thus, highly specialised nanomaterial systems (e.g. membranes, proteins, DNA) exploit non-covalent intermolecular and/or intramolecular interactions. These interactions govern the construction of suprastructures able to perform highly specialised functions such as containers, mechanical machineries and even information storage and transmission.[1] Similarly, artificial complex architectures are obtained by means of supramolecular chemistry[2] where the achievement of well-defined functional nanostructures is given by a spontaneous but controlled self-organization process which represents a nature-mimicking approach to nanotechnology.[3] Among the many examples reported, the spontaneous self-organisation in diluted conditions of amphiphilic block copolymers provides a simple way to construct nanocontainers by a supramolecular mechanism (e.g. polymeric micelles and polymersomes) for biological applications.[4]

The adoption of controlled radical polymerisation techniques[5] such as NMP (Nitroxide Mediated Polymerisation), ATRP (Atom Transfer Radical Polymerisation)[6] and RAFT (Radical Addition-Fragmentation chain Transfer)[7] allowed the synthesis of well defined amphiphilic block copolymers composed by the most varied monomers. In particular, RAFT technique has been extensively utilised in bioapplications[8] because of the absence of metal contaminants and for the easily obtainable thiol ended polymers which are suitable for various reversible and irreversible conjugations.[9] Polymeric micelles are capable of enhancing the systemic bioavailability of poorly soluble and easily metabolisable drugs which can also be delivered by passive and active targeting.[10] Furthermore, this kind of nanoparticles are characterised by a high stability, which is necessary to maintain their structural integrity before the delivery. However, this stability should be modulated in order to release the therapeutic agent after the internalisation into the diseased cells. The most feasible internalisation pathway for nanoparticles is certainly by endocytosis to form endocytic vesicles (early endosomes) which undergo progressive acidification.[11] These vacuoles should release their contents to the cytosol in order to exert the desirable therapeutic effect before their transformation into the highly degrading lysosomes (late endosomes). Many strategies have been tested to enhance the early release of the drugs to the cytosol[12] (e.g. pores formation by cationic amphiphilic peptides[13] or membrane disruption by endosomal escape peptides[14]). Among them, the pH-buffering effect (proton sponge effect) of protonable species represents a simple but effective approach. Polymers bearing amino groups are turned, after internalisation, into their polyelectrolytic form determining water afflux by osmosis, as the endosomal environment become progressively more acidic. The consequent swelling causes the rupture of the membrane and the release of the endosomes' contents.[15]

Post-polymerisation modifications of reactive polymers have recently attracted the attention of an increasing number of researchers. These techniques make possible the synthesis of new materials composed by unconventional monomers starting from a single polymeric precursor with defined structures, architectures and ends functionalisations.[16,17] In this light, poly(glycidyl methacrylate) (PGMA) is a very interesting and versatile polymer that facilitates the synthesis of more and more new cost-effective functional materials such as micelles, polymeric capsules, organic–inorganic hybrid materials, polymeric nanoparticles

based on polyion complexes which can be exploited for the delivery of drugs and nucleic acids.[18] We have recently developed a method for the transformation of homo and copolymers of PGMA by treatment with numerous nucleophiles in order to obtain polymers with different properties without altering their original linearity.[19] In particular, the treatment with morpholine yielded poly(2-hydroxy-3-morpholinopropyl methacrylate) (PHMPMA) which is a very promising polymer with a broad solubility ranging from organic solvents to water. N-substituted morpholine compounds are characterised by a $pK_a \cong 7$, this makes the morpholine-modified PGMA a polymer potentially sensitive to physiological pH changes. Furthermore, the hydroxy group present in each repeating unit, besides increasing the affinity with water, is exploitable for additional functionalization.[17,20] Through the developed methodology we have easily obtained amphiphilic block copolymers composed of PHMPMA as the hydrophilic block and of different hydrophobic blocks. These polymers have shown to be capable of self-assembling into core-shell nanoparticles.

We also have a strong background in the synthesis of thiophene-based fluorophores (TFs) for biological applications. TFs are chemically and optically stable compounds, easy to synthesize and characterised by bright fluorescence which is tunable over the entire visible wavelength range.[21] We have employed TFs for the staining of proteins, DNA and live cells[22] and shown that some of them are capable of spontaneously cross the cell membrane and co-assemble with specific proteins through a physiological process leading to the formation of fluorescent and conducting microfibers.[23,24] We have also demonstrated the feasibility of Förster resonance energy transfer (FRET) experiments for monitoring the hybridization of oligonucleotide probes labelled with TFs to a complementary single-stranded DNA target[25] and for the fine tuning of emission colors of silica nanoparticles doped with TFs.[26] FRET - a process by means of which energy is non-radiatively transferred from a donor fluorophore to an acceptor fluorophore distant a few nm - is a very useful tool in bioapplications[27] such as, for example, the very recently reported release of camptothecin from nanoparticles.[28]

In this study, we apply the procedure for the post-polymerisation modification of PGMA to easily obtain the amphiphilic block copolymer (2-hydroxy-3-morpholinopropyl methacrylate)-*b*-poly (methyl methacrylate) (PMMA-*b*-PHMPMA) that is capable of self-assembling into micelles. This amino-polymer, which is responsive to the relatively low pH of the endosomes, can achieve a double function. The first one is to reduce the stability of the micelles after endocytosis with subsequent release of the carried agents from the particles. Then, the protonation of the morpholine nitrogen present in each repeating unit can allow, by means of the "proton sponge effect", the disruption of the early endosomes with delivery of their contents to the cytosol. Another interesting feature of PHMPMA is given by its high hydration that confers to the micelles' shells the needed antifouling property that can reduce the protein absorption upon systemic administration.[29]

The obtained micelles are utilised as vessels for various lipophilic fluorescent oligothiophenes that are then administered to tumour cells, thus promoting their exploitation as tracking systems to monitor the delivery of drugs with low uptake capacity. In this regard, for these preliminary cellular studies, we used a human model of ovarian carcinoma (IGROV-1), that is a type of malignancy with high frequency of relapse due to acquired chemoresistance. To verify the release of properly selected TFs the disappearing of the FRET phenomenon upon cells internalisation has been monitored.

Experimental section

Materials

Glycidyl methacrylate (GMA) (Sigma-Aldrich) was filtered through alumina. Methyl methacrylate (MMA) was flash distilled. 2,2'-Azobis(2-methyl-propionitrile) (AIBN) (Sigma-Aldrich) was crystallized from methanol. 2,2′-Azobis(2,4-dimethylpentanenitrile) (DuPont) was used as received. 2,2′-Dipyridyl disulfide, morpholine, N-methyl pyrrolidone, THF were purchased from Sigma-Aldrich and used as received. Compounds 4-6 have already been described.[20] Compounds 7-9 were synthesized according to well known methodologies[30] and the synthetic details will be reported elsewhere. The dialysis tube (cutoff 12000–14000 Dalton) was purchased from Medicell International Ltd. The cell lines IGROV-1 was a kind gift from INT, (Milano, Italy). Cells were routinely maintained in RPMI medium supplemented with L-glutamine (2 mM), penicillin (100 units mL-1), streptomycin (100 mg mL-1), and 10% heat-inactivated fetal bovine serum (FBS). Cells were maintained at 37°C in a water-saturated atmosphere of 5% CO_2 in air.

Instrumentation details

^{1}H-NMR spectra were recorded at 400 MHz on a Varian Mercury 400. The polymer's molar mass and its distribution (PDI) were determined using a Gel Permeation Chromatography (GPC) instrument (MSI Concept PU III with a refractive index detector Shodex RI-71) equipped with PLgel 5 µm MIXED-D, 300 x 7.5 mm column calibrated with polystyrene standards. Dynamic Light Scattering (DLS) measurements were taken with a Brookhaven NanoBrook Omni Particle Size Analyzer. UV-Vis spectra were recorded using a Perkin Elmer Lambda 20 spectrometer. Photoluminescence spectra were obtained from a Perkin Elmer LS50 spectrofluorimeter exciting at a wavelength corresponding to the maximum absorption. Confocal Laser Scanning Microscopy (CLSM) images were taken using Olympus FV-1000 microscope. Atomic Force Microscopy (AFM) imaging was performed using a Nanoscope Multimode 8 (Bruker, Santa Barbara, USA) equipped with a 15 µm piezoelectric scanner. The AFM was operated in tapping mode and in peak-force tapping mode.

Synthesis of 2-cyano-4-methylpentan-2-yl dithioisonicotinate

The reaction was performed following the procedure previously described for 2-cyanoprop-2-yl dithioisonicotinate.[31] A solution of triphenylmethyl dithioisonicotinate (1.4 g, 3.5 mmol) and 2,2′-azobis(2,4-dimethylpentanenitrile) (1.13 g, 4.55 mmol) in ethyl acetate (120 mL) was degassed in a round-bottom flask equipped with condenser and magnetic stirring and then refluxed for 16 h. The end of the reaction was checked by TLC. After the solvent was removed under vacuum, the crude product was purified by flash chromatography (eluent, ethyl ether). A red oil (0.72 g,

yield 78%) was obtained. ^{1}H NMR (400 MHz, $CDCl_3$), δ:[1.08 (d, J = 7.5 Hz, 3H); 1.13 (d, J = 6.5 Hz, 3H) ($CH(CH_3)_2$)]; [1.90 (dd, ^1J = 14 Hz, ^2J = 5.5 Hz, 1H); 2.22 (dd, ^1J = 14 Hz, ^2J = 6.5 Hz, 1H) (CH_2)]; 2.07 (m, 1H, CH_2CHMe_2); 1.97 (s, 3H, $C(CH_3)CN$); 7.66 (d, J = 5.8 Hz, 2H, *m*-Ar*H*); 8.71 (d, J = 5.8 Hz, 2H, *o*-Ar*H*). ^{13}C NMR (100 MHz, $CDCl_3$), δ: [23.56; 24.01 ($CH(CH_3)_2$)]; 24.59 ($C(CH_3)CN$); 25.82 (CH_2CHMe_2); 46.30 (*C*MeCN); 46.69 (CH*2*); 118.71 (CMe*C*N); 119.88 (*m*-Ar*C*); 150.26 (*p*-Ar*C*); 150.32 (*o*-Ar*C*); 220.42 (*C*=S).

Synthesis of poly (glycidyl methacrylate)

Glycidyl methacrylate (15 mL, 0.11 mol), the RAFT agent 2-cyano-4-methylpentan-2-yl dithioisonicotinate (46.4 mg, 0.18 mmol) and AIBN (1.44 mg, 8.77×10^{-6} mol) were placed in a 20 mL volumetric flask, toluene was added to fill the flask. The solution was placed in an ampoule which was degassed with four freeze–thaw cycles. The ampoule was placed in a thermostatic bath set at 70 °C. After 3 ½ hours the polymerization was stopped by cooling the ampoule. A sample was taken for the conversion determination by NMR. The polymer was precipitated in ethyl ether twice. The NMR conversion (25%) was calculated by comparing the integral signals of GMA vinyl hydrogens at 5.53 and 6.08 ppm with those at 2.42 – 2.96, 3.16, 3.61 – 4.10 and 4.12 – 4.65 ppm of the glycidyl moiety that are overlapped or partially overlapped in their monomeric/polymeric form. The obtained polymer (3.72 g) was analysed by GPC and showed number average molecular weight ($\overline{M}_n$) of 22600 mol/g with a PDI of 1.13.

Synthesis of poly (glycidyl methacrylate)-*b*-poly (methyl methacrylate)

PGMA macroRAFT (1.23 g, 5.4×10^{-5} mol), MMA (7 mL, 65 mmol) and AIBN (0.44 mg, 2.68×10^{-6} mol) were placed in a 10 mL volumetric flask, that was topped up with dry acetonitrile. The solution was placed in an ampoule which was degassed with four freeze–thaw cycles. The ampoule was placed in a thermostatic bath at 70 °C. After 6 hours the polymerization was stopped by cooling the ampoule. A sample was taken for the conversion determination by NMR. The volatiles were removed in a rotary evaporator under reduced pressure, the residue was dissolved in chloroform and it was precipitated in ethyl ether. The NMR conversion (21%) was calculated by comparing the integral signals of the ester methyl of the monomer (3.71 ppm) with the one of the polymer (3.58 ppm). The obtained polymer (1.9 g) was analysed by GPC and showed a $\overline{M}_n$ of 51000 mol/g with a PDI of 1.19. A more accurate molar mass was estimated by NMR (48600 mol/g) comparing the signal of the ester methyl of PMMA block (3.58 ppm) with the signals of the glycidyl moiety of PGMA block (2.63, 2.84, 3.23, 3.80, 4.29 ppm).

Synthesis of poly (2-hydroxy-3-morpholinopropyl methacrylate)-*b*-poly (methyl methacrylate)

PGMA-*co*-PMMA (1.5 g, 3,1 × 10^{-5} mol) and 2,2′-dipyridyl disulfide (20 mg, 9,1 × 10^{-5} mol) were dissolved in N-methyl pyrrolidone (15 mL). Then morpholine (4.3 mL, 49.6 mmol) was added and the solution was stirred for 30 minutes at room temperature. The ampoule was placed in an oil bath at 80° C and left for two hours. The volatiles were removed in a rotary evaporator at 1 mbar, the residue was dissolved in chloroform and it was precipitated in ethyl ether. After filtration a white powder of PHMPMA-*b*-PMMA (1.8 g) was recovered. Considering the exhaustive reaction of morpholine with the epoxy moieties (see NMR Figure SI-2) the calculated molar mass is 62400 g/mol. GPC analysis gave $\overline{M}_n$ 62000 g/mol PDI 1.19.

Micelles formation

The block copolymer (6 mg) and the fluorophore (0.2 mg) were dissolved in THF (0.5 mL). The vial was stirred by vortex and deionized water (5 mL) was added dropwise. The obtained clear suspension was placed in a dialysis tube which was left in deionized water (refreshed three times) in order to eliminate THF. The aqueous suspension was characterised by DLS measurements, UV-Vis spectroscopy and spectrofluorimetry.

AFM analysis

The samples were prepared by spin coating of a micelle solutions onto freshly cleaved mica. After the deposition, the samples have been kept in a vacuum desiccator for three days in order to remove the aqueous film on the samples. Different starting concentrations of micelles have been tested in order to obtain the best distribution on the mica.

Confocal microscopy analysis

Cells (105) were seeded on coverslips placed in 6-well plates with 2 mL of culture medium. After 24 h incubation at 37 °C the medium was replaced with 2 mL of fresh medium containing micelles at a dilution ratio of 1:20 (33 µg/mL) and incubated either for 3h or 24h. Then, the cells were washed with PBS, fixed with 4% paraformaldehyde, washed with PBS and mounted in glycerol. The confocal imaging was performed on a confocal microscope equipped with an argon laser source (excitation at 405 nm for the green TPs and at 488 nm for the red TPs,) with a DM488/405-type dichroic filter. The acquisition windows were set at different wavelengths according to emission pathways of the tested oligothiophenes. Negative controls consisted of cell samples not incubated with unlabeled micelles.

Cell viability assay

A viability assay (MTT test) was performed using the 3-(4,5-dimethyl-2-thiazolyl)-2,5-diphenyl-2H-tetrazolium bromide on IGROV-1 cells added either with labeled or empty micelles. In details, 5*104 cells were seeded in each well of a 12 well-plate, and after 24h incubation at 37°C, the medium was replaced with fresh medium containing the nanomicelles at different diluitions (1:10 and 1:20). After an additional 24 h of incubation at 37°C, the medium was removed, the cells washed twice with phosphate buffer (pH 7.4), and 1mL of fresh medium serum-free containing 1mg/mL of MTT was added into each well. After 3 h of incubation at 37°C, the MTT, reduced by the mitochondrial reductase of vital cells, formed a dark insoluble product, the formazan. From each well the medium was collected, centrifuged and then discarded. The dark pellet was dissolved in 2mL of DMSO, leading to a violet solution whose absorbance at 570 nm was determined. The absorbance value can be correlated to the percentage of vital cells, by comparing the data of the treated cells with those of the control cells (where no nanomicelles were added).

Cite this: DOI: 10.1039/c0xx00000x

www.rsc.org/xxxxxx

ARTICLE TYPE

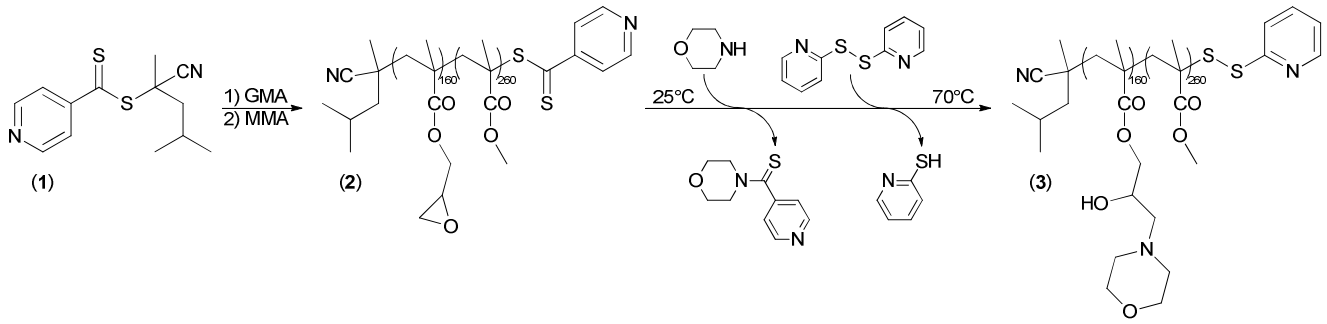

Scheme 1 Synthesis of linear PHMPMA-b-PMMA

Results and discussion

Synthesis of the amphiphilic block copolymer

Poly(glycidyl methacrylate)$_{160}$-*b*-poly(methyl methacrylate)$_{260}$ was synthesised by RAFT polymerisation using 2-cyano-4-methylpent-2-yl dithioisonicotinate (**1**, Scheme 1) as the controlling agent. This RAFT agent was chosen considering its high transfer coefficient towards methacrylates given by the electron withdrawing Z group[31] and the sterically hindered tertiary leaving group,[31,32] in order to obtain well-controlled polymers. The first step consisted in the synthesis of poly(glycidyl methacrylate) (^{GPC}Mn 22600, PDI 1.13) (Figure SI-1) which was subsequently chain-extended with methyl methacrylate. The molar mass of the obtained PGMA-*b*-PMMA block copolymer (**2**, Scheme 1) was measured by GPC and also estimated by comparing the methyl NMR integrals of PMMA block at 3.59 ppm and of the oxirane ring proton at 3.23 ppm (Figure SI-2) ($^{GPC}\overline{M}_n$ 51000, PDI 1.19; $^{NMR}\overline{M}_n$ 49000). The amphiphilic properties were conferred to the synthesised block copolymer by the post-polymerisation treatment with morpholine. In a first step at room temperature, the dithiocarbonyl function is promptly displaced by morpholine (aminolysis) to yield a polymer terminated with a thiol function which, in presence of 2,2'-dipyridyldisulfide (DPDS), quickly react to give a dithiopyridine ended polymer through a thiol exchange reaction (Scheme 1). Upon heating at 80° C, the epoxy functionalities reacted with the excess morpholine (10 fold with respect to epoxy unities) to yield the amphiphilic block copolymer poly(2-hydroxy-3-morpholinopropyl methacrylate)$_{160}$-*b*-poly(methyl methacrylate)$_{260}$ (PHMPMA-*b*-PMMA) where the PGMA block is exhaustively converted into PHMPMA. This block is essential during the micellisation step because it is soluble in water and in polar organic solvents. This feature is given by the hydroxy groups and morpholine moieties present in each repeating unit of the hydrophilic block (**3**, Scheme 1). Another important advantage of the epoxy ring opening reaction is the reactivity of the resulting hydroxy groups which permits additional functionalizations along the chain.[17,19] The instantaneous reaction of the terminal thiol with DPDS prevents side reactions such as polymer dimerisation through disulfane bridge formation or thiol-epoxy interaction. The protection of the thiol group allows the polymer to maintain its original linearity. Moreover, the dithiopyridyl terminal group makes possible further functionalisations (especially bioconjugation) through successive thiol exchange reactions.[33] The proposed post-polymerisation approach represents an optimal way to achieve unconventional - or not otherwise obtainable - amphiphilic block copolymers with the advantage of preventing solubility complications during the polymerisation reactions. At the same time, these polymers, when combined with the RAFT process, can have a controlled and narrow molecular weight, be designed with a specific architecture and also bear heterotelechelic functionalities.[34] In a similar way, other kind of controlled radical polymerisations can take advantage of the post-polymerisation processes of PGMA.

Table 1 DLS average diameter and Z potential (ζ) of empty and loaded micelles in deionised water (pH 5-6).

Micelles-Dye	Diameter (nm)	Z Potential ζ (mV)
M$^{(Empty)}$	25	+30
M-4	25	+21
M-5	30	+24
M-6	90	+30
M-7	30	+20
M-8	30	+22
M-9	40	+21

Micelles self-assembling

The slow addition of water to a THF solution of PHMPMA-*b*-PMMA promotes the formation of the spherical nanoscopic particles by a self-assembling process which is driven by the separation from water of the hydrophobic PMMA blocks. These lipophilic segments tend to minimise the contact surface with the aqueous environment while the hydrophilic PHPMPA blocks provide phase segregation by a thermodynamically controlled process. The balance between the action of the two blocks - and their relative length - determines the micelles' dimension and shape.[35] At the end of the process, the formed spherical core-shell micelles are constituted by a lipophilic nucleus and a hydrated shell. After dialysis in deionised water, for THF removal, the micelles result stable and were analysed by DLS and AFM. Their hydrodynamic diameter and Z potential resulted to be

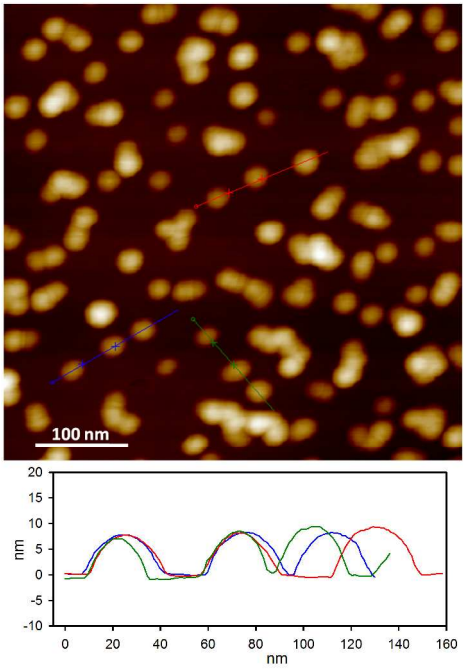

Fig. 1 AFM height image and the respective profiles of the coloured sections.

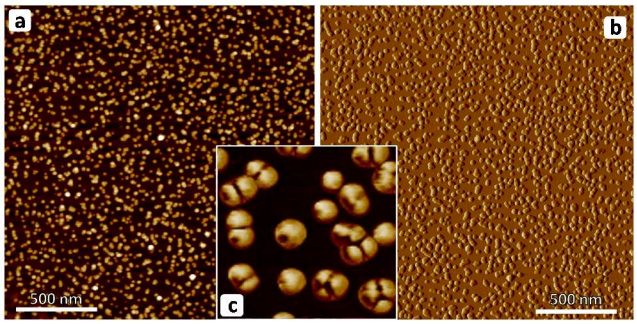

Fig. 2 AFM peak force mode images of height (a) and peak force error (b) for a micelles (1 mg/mL) solution spin-coated on mica immediately after preparation. c) phase image in which can be clearly recognized the contours of the individual micelles forming small agglomerates.

respectively 25 nm and +30 mV (in deionised water which pH value is around 5-6) (Table 1). AFM experiments confirmed the dimension revealed by DLS (Figure 1). The average diameter was 30 nm and the average height was 8 nm; this apparent discrepancy can be explained by the different condition of the deposited-on-surface/dehydrated micelles respect to them in their native aqueous medium. The removal of water from the hydrated shell cause a partial collapse of the hydrophilic blocks resulting in a decreased height while the geometry of the AFM tip slightly increase the diameter. It's also visible the tendency of the deposited particles to stay in close proximity each other although they remain distinct objects (c, Figure 2), this process may be promoted during the deposition of the sample by spin coating deposition and subsequent desiccation. The behaviour of the deposited micelles to form agglomerates without nucleus coalescence reveals their high kinetic stability.[36] This high stability is provided by the PMMA block, which is characterised by a high glass transition temperature (105°C), and can probably ensure the integrity of the supramolecular nanostructure in the cell culture media.[37] The small size of the developed nanoparticles can reduce the recognition by the mononuclear phagocytic system in the spleen and in the liver.[38] Moreover, the highly hydrated shell is considered to provide antifouling properties (anti-nonspecific protein adsorption properties)[28] in order to reduce opsonisation and its consequent macrophage recognition, thus enhancing the permanence in the systemic circulation. This longer blood circulation time, associated with the enhanced permeability and retention effect (EPR) occurring in cancer tissues would provide a more efficient passive targeting of the nanoparticles to neoplasms.

Micelles loaded with fluorophores and their photophysical properties

Lipophilic substances can be incorporated into the micelles during the self-assembling process. To achieve this, the dye and the polymer are dissolved in THF before adding water. After dialysis, the resulting loaded nanoparticles present similar dimension to the empty ones (Table 1). The only exception is given by the charged compound 6 (sulfonyl anion) which, interacting with the partially cationised tertiary amines of the hydrophilic blocks, forms reasonably greater particles. Fluorophores 4-9 (Figure 3) were all easily loaded into the micelles regardless the different structures and molecular weight which spans from 294 to 1857 g/mol. UV-Vis absorption and emission spectra of the fluorophores are reported in Figure 4. The samples loaded into the micelles showed a slight hypsochromic shift which became more evident in the PL emission; this is probably due to molecular distortion caused by confinement.

In two different experiments, the couples of fluorophores 4, 7 and 5, 7 have been loaded into the micelles. Observing their behavior when singularly hosted in micelles, compounds 4 and 5 display an emission maximum respectively at 475 nm and 510 nm, while compound 7 displays an absorption maximum at 480 nm (Figure 4). When the paired structures are in close proximity a FRET phenomenon can be observed. This consists in an energy transfer from the excited state of the donor chromophore to the acceptor chromophore through a nonradiative dipole–dipole coupling. The efficiency of this energy transfer is inversely proportional to the sixth power of the distance between donor and acceptor, making FRET extremely sensitive to small changes in distance. Those pairs have been chosen because of the advantageous matching between the emission of the donor and the absorption of the acceptor (spectral overlap integral J), which maximises the energy transfer process. To verify this phenomenon, the two compounds 5 (76 μM) and 7 (36 μM) were dissolved in THF and analysed by UV-Vis and PL. The absorbance spectrum shows two maximum absorptions at 400 and 500 nm as is expected from the sum of the two compounds, indicating that there are no interactions in the ground state. The PL analysis showed two distinct maximum emission peaks respectively at 550 nm and 680 nm that strongly depend on the excitation wavelength. This resemble the emission bands of the individual compounds. It must be highlighted that, when excited at 400 nm, this two component solution presents only the emission of compound 5 at 550 nm, and, when excited at 500 nm, the characteristic emission of compound 7 at 680 nm is recorded together with a very low emission of compound 5 (Figure 5a). The spectra reported in Figure 5a are normalized in the maxima, but it is worth noting that the fluorescence quantum yield of compound 5 is 12 times

Cite this: DOI: 10.1039/c0xx00000x

www.rsc.org/xxxxxx

ARTICLE TYPE

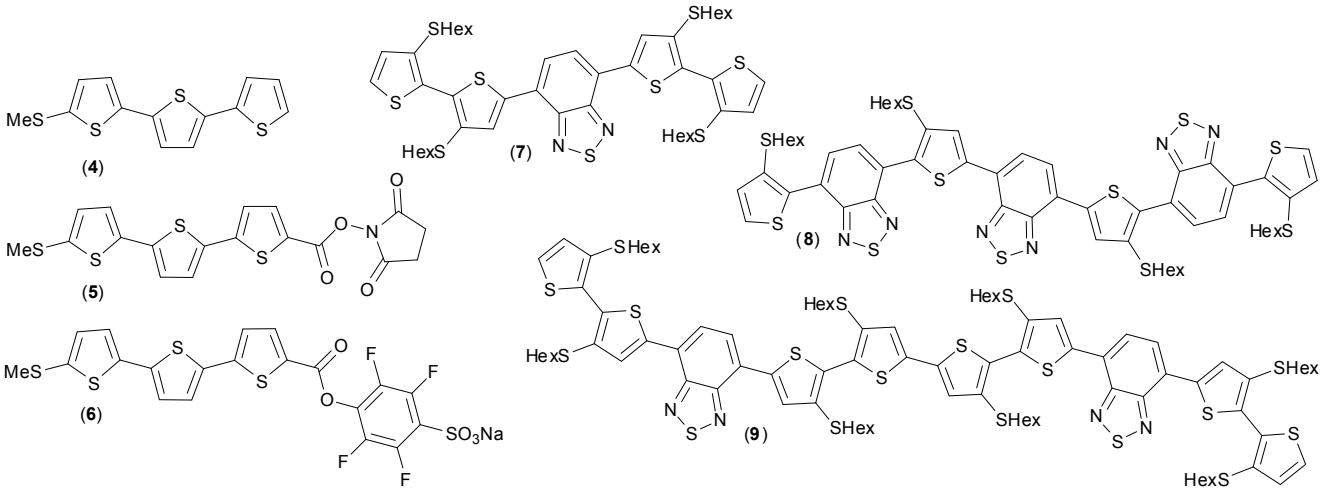

Fig. 3 Oligothiophene based chromophores

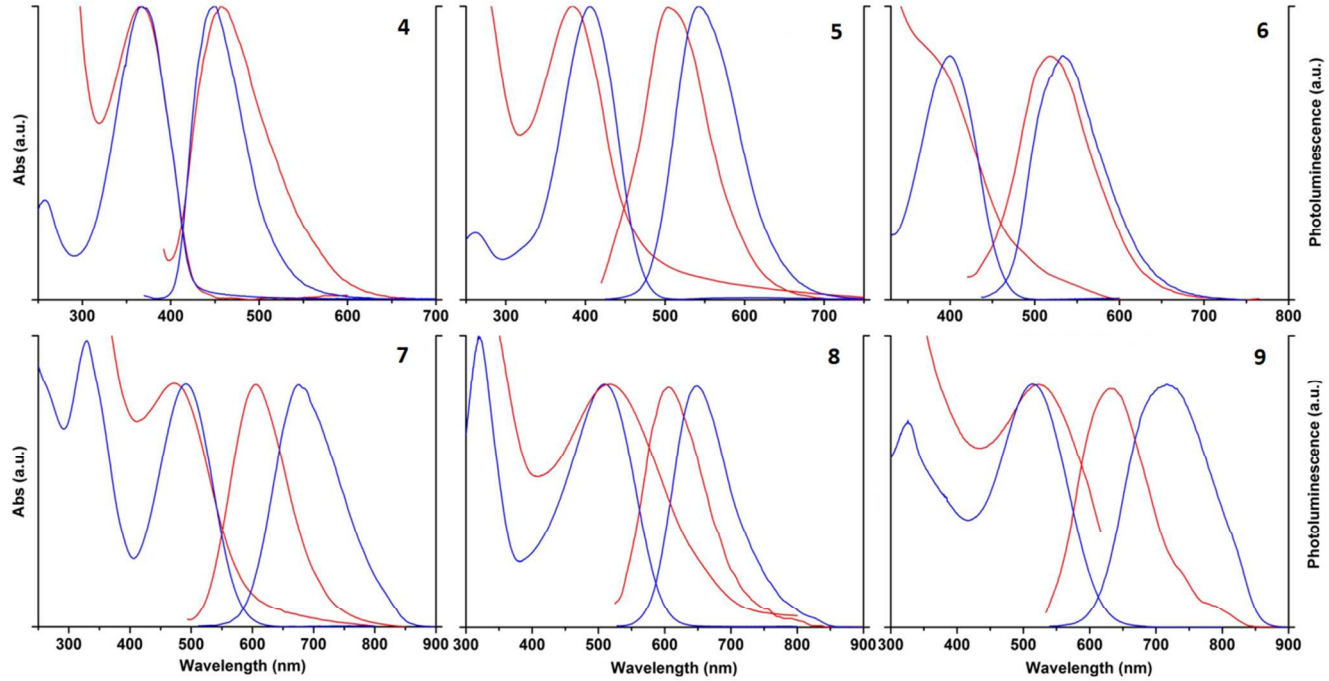

Fig. 4 Normalised absorbance and emission spectra of compounds 4-9. Blue line in THF solution, red line in micelles aqueous suspension.

higher than that of 7 (Φ_5 = 0.51, Φ_7 = 0.04). Conversely, the aqueous suspension of micelles loaded with the same compounds at the same concentration showed two maximum absorptions at 357 and 480 nm, similar to those observed for the fluorophores separately hosted in micelles (Figure 4). Also, the photoluminescence analysis shows, with the excitation wavelength set at 357, a quenched emission at 450 nm (compound 5) and a main peak at 625 nm which overlaps perfectly the emission obtained exciting at 480 nm (compound 7) (Figure 5b). In this case, the very low emission of compound 5, considering its higher molar concentration (2 folds) and its higher quantum yield (12 folds), clearly demonstrates the occurring of FRET within the micelles core. Moreover, the same THF solution and the aqueous suspension were observed under an UV lamp at 365 nm and the FRET phenomenon is evident even to the naked eye. The THF solution shows a very bright green emission that overcome the red emission, while the micelles' suspension shows only the characteristic red emission of compound 7 (Figure 6).

Cite this: DOI: 10.1039/c0xx00000x

www.rsc.org/xxxxxx

ARTICLE TYPE

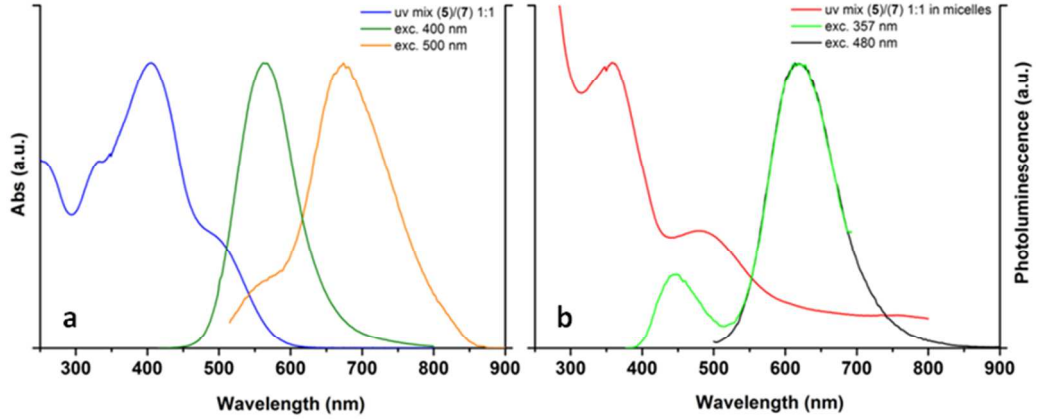

Fig. 5 Normalised absorbance and emission spectra of compounds 5 and 7 in THF solution (a) or in micellar suspension (b).

Fig. 6 Light emission of compounds 5 and 7 in THF solution (left) and in micellar aqueous suspension (right) under UV lamp exposition (365 nm).

These two component suspensions have been utilised to verify if the micelles release their contents upon cells uptake.

Administration of the loaded micelles to cultured cells

IGROV-1 cells were incubated with micelles loaded with the selected TFs and monitored by CLSM at fixed time-points in order to study the time course of micelles internalization and subcellular localization. All the TFs loaded micelles undergo a rapid internalization in the tested cells. Indeed, after 3 hours incubation cells look bright, especially for the green emitting fluorophores, and fluorescent spots are visible in the cytosol (Figure 7). The only exception is given by micelles loaded with compound 6 which resulted to be greater in size (Table 1). The different dimension can be responsible for the slower internalization rate.

In the case of the micelles loaded with red emitting TFs, the fluorescence signal resulted to be less intense especially for the higher molecular weight compounds. This is due by the different molar concentration of the fluorophores for each kind of micelles suspension as we loaded the same amount in mass (200 μg) for all of the samples (0.11 μM – 0.018 μM) and also by the reduction of the fluorescence quantum yield that occurs extending the conjugation system.

The images taken with CLSM show that the fluorophores are mainly localized in the perinuclear region of the cells, where both the endoplasmic reticulum and Golgi apparatus are located. The maximum fluorescence intensity was reached after 24 h of incubation, even if the labelled micelles were promptly incorporated into IGROV-1 cells within the first 3 h (Figure 7). These findings show that, regardless of the type of TFs loaded within the micelles, the fluorescence intensity and distribution inside the cells is almost the same, thus reinforcing the concept that the carrier, and not TFs, is the key factor that drives the uptake pathway. The internalization process that is used by cells to incorporate micelles is certainly by endocytosis.[10,11] Among the different endocytosis mechanisms, adsorptive endocytosis[39] may be involved in this case because the tertiary amines present in the micelles' shell are partially charged. The interaction, in the acidic environment of tumor tissues, between the positive charged corona (ζ = +20 – +30 mV) of the particles and the negative charged plasma membrane - which triggers endocytosis - is probably responsible for this internalization pathway.[40] Another advantage brought by the tertiary amines, which are present in each repeating unit of the hydrophilic polymer block, is

Cite this: DOI: 10.1039/c0xx00000x

www.rsc.org/xxxxxx

ARTICLE TYPE

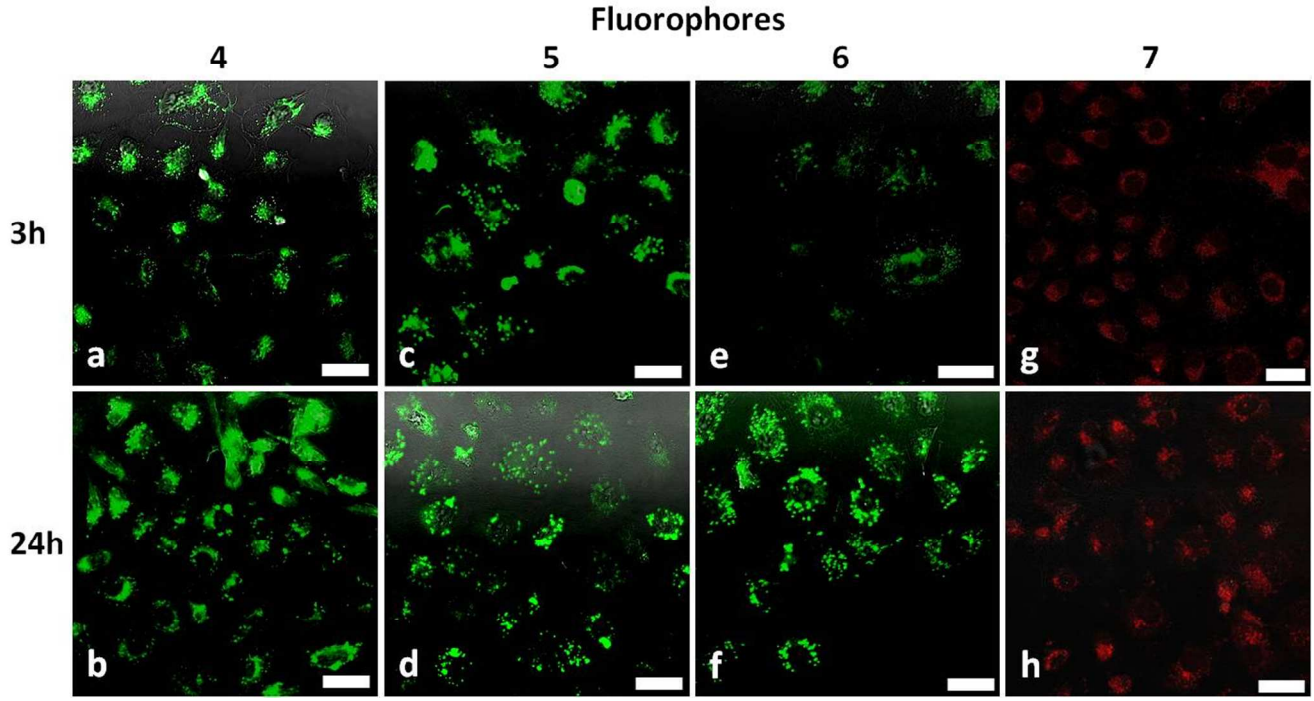

Fig. 7 Confocal laser scanning microscopy images of IGROV-1 cells incubated for 3 and 24 hours with TFs loaded micelles. Scale bars 25 micron.

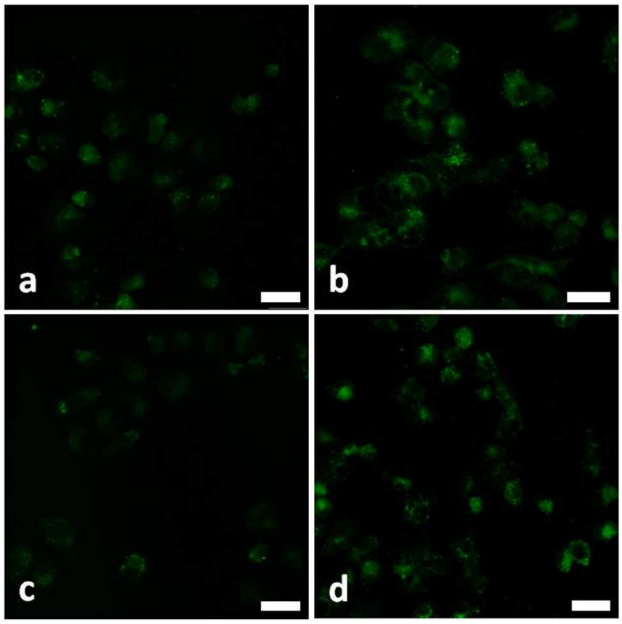

Fig. 8 Confocal laser scanning microscopy images of IGROV-1 cells incubated for 3 (a, c) and 24 (b, d) hours with the naked TFs **4** (a, b) and **5** (c, d). Scale bars 25 micron.

given by the "sponge-effect" that can lead to the breakage of the endocytic membrane. This causes the release of the endosomes contents that would occur before they are converted into the highly degrading lysosomes. The endosomal pH decrease promotes a high protonation of PHMPMA, which, besides destabilising the micelles, results in an osmotic swelling due to water entry and subsequent vacuole disruption.[41] It has also been reported that the swelling of the polymer network, due to an increasing repulsion between the protonated chains, can enhance the release from the endosome by a similar mechanism.[42] The endosomal escape and therapeutic efficacy of drugs loaded into the developed micelles will be investigated in future work.

A control set of experiment was performed by administering the TFs using DMSO as dispersant media. The internalization rate resulted to be much slower without the carrier as, after three hours, the fluorescence is barely perceptible and a bit more intense after 24 hours (Figure 8). The insolubility of the fluorophores in the aqueous cell media suggests that they can be internalised by macropinocytosis[43] which is a highly active non-specific internalization mechanisms in cancer cells.

The micelles, loaded with the FRET-paired green and red TFs, have also been tested to demonstrate the release of their contents within cells and their codelivery ability. CLSM experiments were performed by acquiring separately the emission of the green and red fluorophores and the two images were merged (Figure 9). It is clearly visible that the two TFs are colocalised, and, more importantly, the green color is predominant as it happens when they are in solution (Figure 6). This means that, although the fluorophores reside in the same subcellular compartment, the FRET phenomenon is not occurring thus demonstrating the

Cite this: DOI: 10.1039/c0xx00000x

www.rsc.org/xxxxxx

ARTICLE TYPE

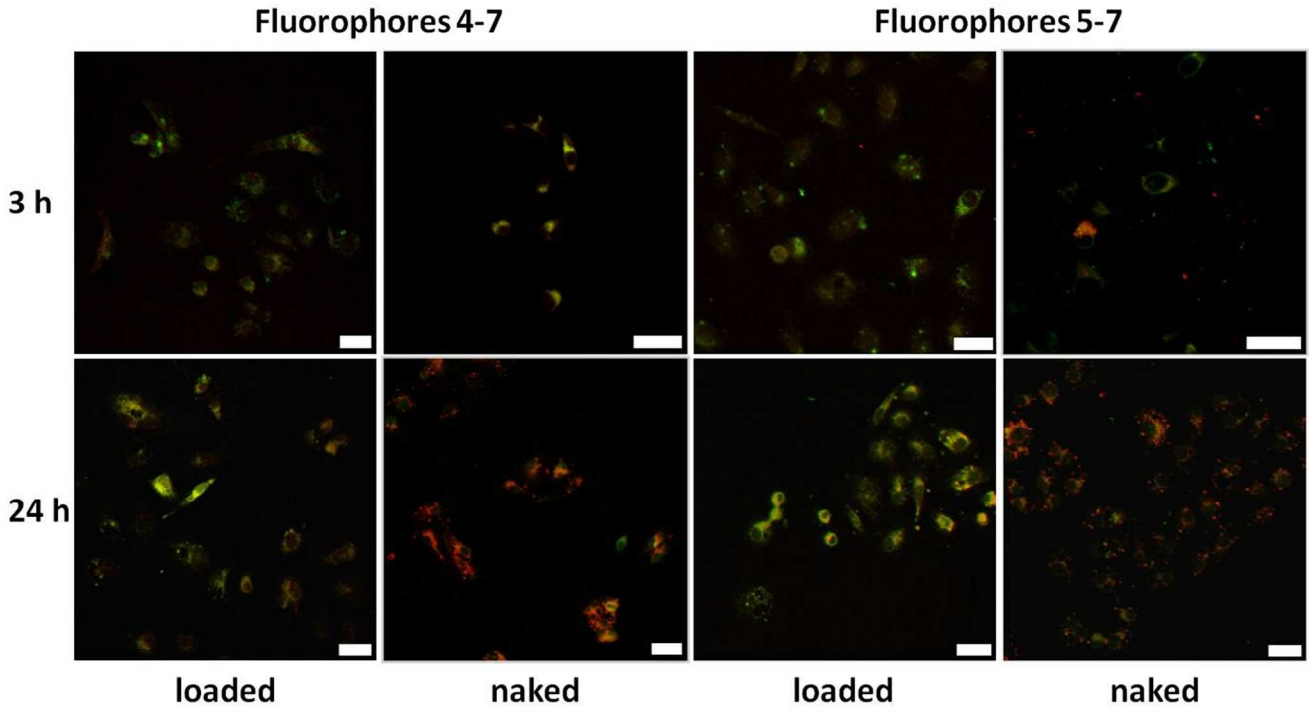

Fig. 9 Confocal laser scanning microscopy images of IGROV-1 cells incubated for 3 and 24 hours with a mixture of green and red emitting TFs (loaded in micelles or naked). Scale bars 25 micron.

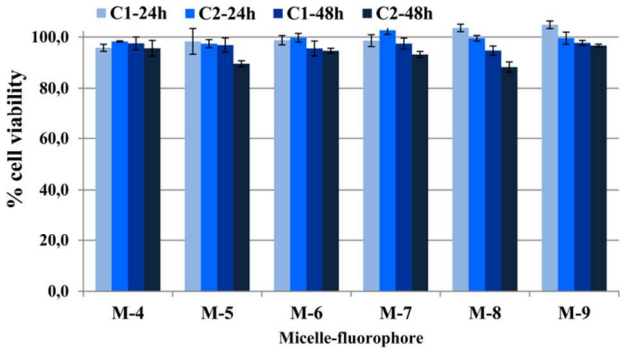

Fig. 10 IGROV-1 cells viability incubated with TFs loaded micelles using two different concentration (C1 dilution 1/20; C2 dilution 1/10). The assay was performed after 24 and 48 h of continuous incubation. Each data point is triplicated.

release of the micelles' contents. Conversely, the administration of the same two mixtures suspended by DMSO leads to different results. It is noticeable in this case, the separation of the two TFs, especially after 24 hours. This behavior suggests that they might be uptaken by the cells by similar internalization pathways but, at 24 hours, the fluorophores show an increased separation. This can be explained by a process of molecular recognition during which the different structures of the oligothiophenes recognise different proteins by their secondary and tertiary structures.[21,44] This peculiar characteristic of oligothiophenes is given by their ability of deforming and adapting their structure to the surrounding environment.[45]

MTT assays were also conducted and no toxicity was revealed for the fluorophores loaded micelles (Figure 10).

Conclusions

A new generation of amphiphilic block copolymers have been developed. They are capable of self-assembling into very robust micelles and can load lipophilic substances. Different water-insoluble oligothiophene fluorophores were dispersed in water by means of the nanoparticles obtaining light emitting aqueous suspensions. Moreover, pairs of selected green and red emitting TFs were loaded and a FRET phenomenon was observed. The loaded micelles were administered to IGROV-1 cells and a rapid internalisation - and release - of the fluorophores was observed by CLSM. Neither the polymeric vessels nor the oligothiophenes have shown cytotoxicity towards the tested cells. This new polymeric material is able to generate micelles with adaptable stability that can make possible the delivery to the diseased tissue and, subsequently, the release within cells of lipophilic substances such as fluorescent compounds. They are also able to codeliver structurally different substances for diagnostic - and reasonably also for therapeutic - purposes, thus meeting the criteria of theranostic approach.

Notes and references

[a] *Istituto per la Sintesi Organica e la Fotoreattività, Consiglio Nazionale delle Ricerche, Area della Ricerca, via P. Gobetti, 101, 40129 Bologna, Italy. Fax: +39 051 6398349; Tel:+39 051 6398257; E-mail: massimo.benaglia@cnr.it*

[b] *Istituto di Nanotecnologia, Consiglio Nazionale delle Ricerche, Polo di Nanotecnologia c/o Campus Ecotekne, via Monteroni - 73100 Lecce.*

[c] *Dipartimento di Chimica "G. Ciamician", University of Bologna, Via Selmi 2, 40126, Bologna (Italy) Fax: +39 051 2099456 E-mail: giacomo.bergamini@unibo.it*

[d] *Dipartimento di Chimica Industriale "Toso Montanari" and INSTM UdR-Bologna, University of Bologna, Viale Risorgimento 4, 40136 Bologna, Italy. Fax: +39 051 2093675; Tel.: +39 051 2093688. E-mail: loris.giorgini@unibo.it*

† Electronic Supplementary Information (ESI) available: GPC chromatograms and NMR spectra of the synthesised polymers. See DOI: 10.1039/b000000x/

1 J. M. Lehn, *Angew. Chem. Int. Ed.* 1990, **29**, 1304-1319.
2 a) J. M. Lehn, *Angew. Chem. Int. Ed.* 1988, **27**, 89-112. b) D. Philp, J. F. Stoddart, *Angew. Chem. Int. Ed.* 1996, **35**, 1154-1196. c) M. C. T. Fyfe, J. F. Stoddart, *Acc. Chem. Res.* 1997, **30**, 393-401.
3 J. M. Lehn, *Proc. Natl. Acad. Sci. U.S.A.*, 2002, **99**, 4763-4768.
4 a) A. Harada, K. Kataoka, *Prog. Polym. Sci.* 2006, **31**, 949-1038. b) Z. L. Tyrrell, Y. Q. Shen, M. Radosz, *Prog. Polym. Sci.* 2010, **35**, 1128-1143. c) M. Benaglia, A. Alberti, E. Spisni, A. Papi, E. Treossi, V. Palermo, *J. Mater. Chem.*, 2011, **21**, 2555-2562.
5 J. F. Lutz, *Polym. Int.*, 2006, **55**, 979-993.
6 K. Matyjaszewski and N. V. Tsarevsky, *Nat. Chem.*, 2009, **1**, 276-288.
7 a) G. Moad, E. Rizzardo and S. H. Thang, *Aust. J. Chem.*, 2005, **58**, 379–410; b) G. Moad, E. Rizzardo and S. H. Thang, *Aust. J. Chem.*, 2006, **59**, 669–692; c) G. Moad, E. Rizzardo and S. H. Thang, *Aust. J. Chem.*, 2009, **62**, 1402–1472.
8 (a) A. W. York, S. E. Kirkland and C. L. McCormick, *Adv. Drug Deliv. Rev.* 2008, **60**, 1018–1036. (b) C. Boyer, V. Bulmus, T. P. Davis, V. Ladmiral, J. Liu, and S. Perrier, *Chem. Rev.* 2009, **109**, 5402–5436.
9 P. J. Roth, C. Boyer, A. B. Lowe, T. P. Davis, *Macromol. Rapid Commun.* 2011, **32**, 1123-1143.
10 Y. Lu and K.Park, *Int. J. Pharm.*, 2013, **453**, 198-214.
11 H. Hillaireau and P. Couvreur, *Cell. Mol. Life Sci.*, 2009, **66**, 2873-2896.
12 (a) L. Y. T. Chou, K. Ming and W. C. W. Chan, *Chem. Soc. Rev.*, 2011, **40**, 233-245. (b) A. K. Varkouhi, M. Scholte, G. Storm and H. J. Haisma, *J. Control. Release*, 2011, **151**, 220-228.
13 H, W, Huang, F. Y. Chen and M. T. Lee, *Phys. Rev. Lett.*, 2004, **92**, 198304.
14 N. M. Moore, C. L. Sheppard, T. R. Barbour and S. E. Sakiyama-Elbert, *J. Gene Med.*, 2008, **10**, 1134-1149.
15 C. Lin and J.F. Engbersen, *J. Control. Release*, 2008, **132**, 267–272.
16 K. A. Gunay, P. Theato and H. A. Klok, *J. Polym. Sci. A Polym. Chem.* 2013, **51**, 1-28.
17 (a) S. De and A. Khan, *Chem. Commun.*, 2012, **48**, 3130–3132. (b) S. De, C. Stelzer and A. Khan, *Polym. Chem.*, 2012, **3**, 2342-2345.
18 Q. L. Li, W. X. Gu, H. Gao and Y. W. Yang, *Chem. Commun.*, 2014, **50**, 13201-13215.
19 M. Benaglia, A. Alberti, L. Giorgini, F. Magnoni and S. Tozzi, *Polym. Chem.*, 2013, **4**, 124–132.
20 H. Kakwere and S. Perrier, *Polym. Chem.*, 2011, **2**, 270–288.
21 M. Zambianchi, F. Di Maria, A. Cazzato, G. Gigli, M. Piacenza, F. Della Sala and G. Barbarella, *J. Am. Chem. Soc.*, 2009, **131**, 10892-10900.
22 (a) M. Duca, B. Dozza, E. Lucarelli, S. Santi, A. Di Giorgio and G. Barbarella, *Chem. Commun.*, 2010, **46**, 7948-7950. (b) M. L. Capobianco, G. Barbarella and A. Manetto, *Molecules*, 2012, **17**, 910-933. (c) F. Di Maria, I. E. Palamà, M. Baroncini, A. Barbieri, A. Bongini, R. Bizzarri, G. Gigli, and G. Barbarella, *Org. Biomol. Chem.*, 2014, **12**, 1603-1610.
23 I. Palamà, F. Di Maria, I. Viola, E. Fabiano, G Gigli, C. Bettini and G. Barbarella, *J. Am. Chem. Soc.*, 2011, **133**, 17777-17785.
24 I. E. Palamà, F. Di Maria, S. D'Amone, G. Barbarella and G. Gigli, *J. Mater. Chem. B*, 2015, **3**, 151-158.
25 G. Barbarella, M. Zambianchi, A. Ventola, E. Fabiano, F. Della Sala, G. Gigli, M. Anni, A. Bolognesi, L. Polito, M. Naldi and M. L. Capobianco, *Bioconjugate Chem*. 2006, **17**, 58-67.
26 M. Melucci, M. Zambianchi, G. Barbarella, I. Manet, M. Montalti, S. Bonacchi, E. Rampazzo, D. C. Rambaldi, A. Zattoni and P. Reschiglian, *J. Mater. Chem.* 2010, **20**, 9903-9909.
27 (a) K. E. Sapsford, L. Berti and I. L. Medintz, *Minerva Biotecnol.*, 2004, **16**, 247-273. (b) S. Jingyu, T. Feng, L. Jing and Y. Mo, *J. Mater. Chem. B*, 2015, Advance Article, DOI: 10.1039/c5tb00885a.
28 H. Wang, M. Xu, M. Xiong and J. Cheng, *Chem. Commun.*, 2015, **51**, 4807-4810.
29 L. Liu, W. Li and Q. Liu, *WIREs Nanomed Nanobiotechnol*, 2014, **6**, 599–614.
30 F. Di Maria and G. Barbarella, *J. Sulfur Chem*, 2013, **34**, 627-637.
31 M. Benaglia, E. Rizzardo, A. Alberti and M. Guerra, *Macromolecules*, 2005, **38**, 3129-3140.
32 Y. K. Chong, J. Krstina, T. P. T. Le, G. Moad, A. Postma, E. Rizzardo and S. H. Thang, *Macromolecules*, 2003, **36**, 2256-2272.
33. C. Boyer, J. Liu, V. Bulmus and T. P. Davis, *Aust. J. Chem.*, 2009, **62**, 830–847.
34 (a) C. Boyer, J. Liu, V. Bulmus, T. P. Davis, C. Barner-Kowollik and M. H. Stenzel, *Macromolecules*, 2008, **41**, 5641-5650. (b) C. Boyer, V. Bulmus and T. P. Davis, *Macromol. Rapid Commun.*, **30**, 493-497.
35 L. Zhang and A. Eisenberg, *J. Am. Chem. Soc.*, 1996, **118**, 3168–3181.
36 Y. Wang, J. He, C. Liu, W. H. Chong, and H. Chen, *Angew. Chem. Int. Ed.*, 2015, **54**, 2022–2051.
37 R. Nagarajan, *J. Colloid Interface Sci.* 2015, **449**, 416–427.
38 E. Groves, A. Dart, V. Covarelli and E. Caron, *Cell. Mol. Life Sci.*, 2008, **65**, 1957–1976.
39 S. Mao, O. Germershaus, D. Fischer, T. Linn, R. Schnepf and T. Kissel, *Pharm. Res.*, 2005, **22**, 2058-2068.
40 a) M. Huang, Z. Ma, E. Khor and L. Lim, *Pharm. Res.*, 2002, **19**, 1488-1494. b) O. Harush-Frenkel, N. Debotton, S. Benita and Y. Altschuler, *Biochem. Biophys. Res. Commun.*, 2007, **353**, 26-32.
41 O. Boussif, F. Lezoualc'h, M. A. Zanta, M. D. Mergny, D. Scherman, B. Demeneix and J. P. Behr, *Proc. Natl. Acad. Sci. USA*, 1995, **92**, 7297-7301.
42 J. P. Behr, *Chimia*, 1997, **51**, 34-36.
43 S. Mukherjee, R. N. Ghosh, F. R. Maxfield, *Physiol. Rev.*, 1997, **77**, 759-803.
44 F. Di Maria, I. E. Palamà, M. Baroncini, A. Barbieri, A. Bongini, R. Bizzarri, G. Gigli and G. Barbarella, *Org. Biomol. Chem.*, 2014,**12**, 1603-1610.
45 (a) G. Barbarella, M. Melucci, G. Sotgiu, *Adv. Mater.*, 2005, **17**, 1581-1593. (b) F. Di Maria, P. Olivelli, M. Gazzano, A. Zanelli, M. Biasiucci, G. Gigli, D. Gentili, P. D'Angelo, M. Cavallini and G. Barbarella, *J. Am. Chem. Soc.*, 2011, **133**, 8654-8661.

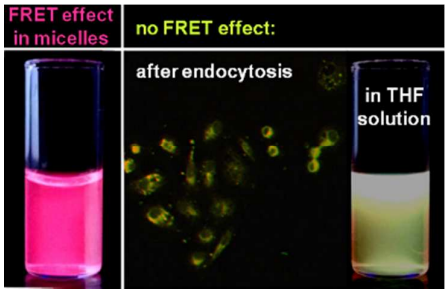

The disappearing of FRET effect upon cells internalisation demonstrates the release from the micelles of the loaded fluorophores.